# 1,2,4-Triazole-3-thione compounds with a 4-ethyl alkyl/aryl sulfide substituent are broad-spectrum metallo-b-lactamase inhibitors with re-sensitization activity

Alice Legru, Federica Verdirosa, Jean-François Hernandez, Giusi Tassone, Filomena Sannio, Manuela Benvenuti, Pierre-Alexis Conde, Guillaume Bossis, Caitlyn A Thomas, Michael Crowder, et al.

# 1,2,4-Triazole-3-thione compounds with a 4-ethyl alkyl/aryl sulfide substituent are broad-spectrum metallo-β-lactamase inhibitors with re-sensitization activity

Alice Legru,[a‡] Federica Verdirosa,[b‡] Jean-François Hernandez,[a*] Giusi Tassone,[c] Filomena Sannio,[b] Manuela Benvenuti,[c] Pierre-Alexis Conde,[a] Guillaume Bossis,[d] Caitlyn A. Thomas,[e] Michael W. Crowder,[e] Melissa Dillenberger,[f] Katja Becker,[f] Cecilia Pozzi,[c] Stefano Mangani,[c] Jean-Denis Docquier[b,g*] and Laurent Gavara[a*]

[a]*IBMM, CNRS, Univ Montpellier, ENSCM, Montpellier, France.* [b]*Dipartimento di Biotecnologie Mediche, Università di Siena, 53100 Siena, Italy.* [c]*Dipartimento di Biotecnologie, Chimica e Pharmacia, Università di Siena, 53100 Siena, Italy.* [d]*IGMM, Univ Montpellier, CNRS, Montpellier, France.* [e]*Department of Chemistry and Biochemistry, Miami University, Oxford, OH, United States of America.* [f]*Chair of Biochemistry and Molecular Biology, Interdisciplinary Research Center, Justus Liebig University, D-35392 Giessen, Germany.* [g]*Centre d'Ingénierie des Protéines-InBioS, Université de Liège, B-4000 Liège, Belgium.*

‡These authors contributed equally.

*Corresponding authors: Tel.: +33-(0)4 11 75 96 08; Fax: +33-(0)4 11 75 96 41.
*E-mail addresses:* laurent.gavara@umontpellier.fr (L. Gavara); jean-francois.hernandez@umontpellier.fr (J.-F. Hernandez); jddocquier@unisi.it (J.-D. Docquier).

**Keywords:** Metallo-β-Lactamase inhibitor; 1,2,4-triazole-3-thione; bacterial resistance; β-lactam antibiotic; thioether.

**Abbreviations list**

*Boc*, *tert*-butyloxycarbonyl; *CFU*, colony-forming unit; *CLSI*, Clinical and Laboratory Standards Institute; *DMF*, dimethylformamide; *DMSO*, dimethylsulfoxide; *DMEM*, Dulbecco's Modified Eagle Medium; *DOR*, doripenem; *DPT*, dipyridyl thionocarbamate; *ETP*, ertapenem; *hGloII*, human Glyoxalase II; *HeLa*, tumoral cells from Henrietta Lacks; *HEPES*, 4-(2-Hydroxyethyl)-1-piperazine-ethanesulfonic acid; *IMP*, imipenemase; *IPM*, imipenem; *KPC*, *Klebsiella pneumoniae* Carbapenemase; *LC-MS*, liquid chromatography coupled to mass spectrometry; *LDH*, Lactate DeHydrogenase; *MBL*, metallo-β-lactamase; *MEM*, Meropenem; *MHB*, Mueller-Hinton broth; *MIC*, Minimum Inhibitory Concentration; *MOPS*, 4-Morpholinopropane sulfonate; *NDM*, New Delhi Metallo-β-lactamase; *OXA*, oxacillinase; *PBMC*, Peripheral Blood Mononucleated Cells; *RPMI*, Roswell Park Memorial Institute medium; *SBL*, serine-β-lactamase; *TFA*, trifluoroacetic acid; *VIM*, Verona Integron-borne Metallo-β-lactamase.

**ABSTRACT**

Metallo-β-lactamases (MBLs) are important contributors of Gram-negative bacteria resistance to β-lactam antibiotics. MBLs are highly worrying because of their carbapenemase activity, their rapid spread in major human opportunistic pathogens while no clinically useful inhibitor is available yet. In this context, we are exploring the potential of compounds based on the 1,2,4-triazole-3-thione scaffold as an original ligand of the di-zinc active sites of MBLs, and diversely substituted at its positions 4 and 5. Here, we present a new series of compounds substituted at the 4-position by a thioether-containing alkyl chain with a carboxylic and/or an aryl group at its extremity. Several compounds showed broad-spectrum inhibition with $K_i$ values in the μM to sub-μM range against VIM-type enzymes, NDM-1 and IMP-1. The presence of the sulfur and of the aryl group was important for the inhibitory activity and the binding mode of a few compounds in VIM-2 was revealed by X-ray crystallography. Importantly, *in vitro* antibacterial susceptibility assays showed that several inhibitors were able to potentiate the activity of meropenem on *Klebsiella pneumoniae* clinical isolates producing VIM-1 or VIM-4, with a potentiation effect of up to 16-fold. Finally, a selected compound was found to only moderately inhibit the di-zinc human glyoxalase II, and several showed no or only moderate toxicity toward several human cells, thus favourably completing a promising behaviour.

## 1. Introduction

Bacterial resistance to antibiotics has reached alarming levels and represents an increasingly important Public Health concern [1-3]. Among the bacterial pathogens responsible of nosocomial infections, carbapenem-resistant Gram-negative bacteria such as Enterobacterales, *Acinetobacter baumannii* and *Pseudomonas aeruginosa* have recently been recognized by the World Health Organization as "critical" priorities for the discovery and development of new antibacterial drugs [4]. Indeed, such organisms are often multi- to extremely-drug-resistant, therefore limiting available treatments to a few therapeutic options [5]. One privileged approach is to restore their susceptibility to carbapenems, which are valuable β-lactam antibiotics considered as last resort antibacterial drugs in the clinical setting.

Among the possible mechanisms of carbapenem resistance, which also include decreased porin expression or efflux, the most relevant is the enzymatic inactivation by β-lactamases endowed with carbapenem-hydrolyzing activity, the so-called carbapenemases. They belong to molecular classes A, B and D of β-lactamases [6,7]. Serine-carbapenemases are active serine enzymes (SBLs) mainly represented by the *Klebsiella pneumoniae* carbapenemases (class A KPC-type enzymes) and the OXA-type class D enzymes such as OXA-48 and OXA-23. Class B β-lactamases have a different catalytic mechanism as they need one or two Zn ion(s) for catalysis, and are further classified into three sub-classes (B1, B2, B3) of so-called metallo-β-lactamases (MBLs) [8,9]. Clinically relevant MBLs include the subclass B1 IMP- (imipenemase), VIM- (Verona integron-borne MBL) and NDM-type (New Delhi MBL) enzymes. They are characterized by a broad substrate profile, an efficient hydrolysis of carbapenems and their insensitivity to currently available SBL inhibitors (clavulanate, avibactam, vaborbactam). These enzyme subtypes are typically encoded by mobile genetic elements (transposons, plasmids) disseminating in Gram-negative fermenters and non-fermenters, which initially emerged and spread in the hospital setting. However, because of their present global dissemination, MBL-producing isolates increasingly cause community-acquired infections [10]. New drugs are urgently needed to fight infections due to MBL-producing bacteria.

Combining a β-lactamase inhibitor with a β-lactam antibiotic is a well-known approach to restore the efficacy of the latter. Several β-lactamase inhibitors are currently marketed (clavulanate, sulbactam, tazobactam, avibactam, vaborbactam) [11,12]. However, they only target some SBLs, including the carbapenemases KPC and OXA-48 in the case of the most recently approved inhibitors [13]. Despite many MBL inhibitors have been reported in the

literature, none have been approved yet [9]. The structural and functional heterogeneity of clinically relevant MBLs represents a true challenge for the discovery of a broad-spectrum inhibitor [14,15]. In addition, most reported inhibitors displayed a zinc-coordinating element in their structures. This element is often determining to reach high affinity and it increases the risk of off-target activity, especially on human metallo-enzymes [16]. It is particularly the case of thiol-containing compounds, which represent the most abundant class of MBL inhibitors described to date [13,17-20]. This potential drawback might be alleviated with rhodanines, which behave as thiol precursors [21,22]. The carboxylate group is another well-known Zn-ligand and compounds containing several of these groups as succinates or dipicolinates were reported [14,23]. Inhibitors with metal-stripping effect as the aspergillomarasmine A [24] or Zn148 [25] also showed potent activity, but they are expected to be of insufficient selectivity. More recently, appeared several families of inhibitors active on both SBLs and MBLs including boronates [26-29], phosphonates [30] and azetidinimines [31]. Only few compounds are currently promising [32]. It includes the thiazole MBL inhibitor ANT2681 [33] and the broad-spectrum inhibitors of MBLs and SBLs cyclic boronates, such as taniborbactam [26,34,35] and QPX7728 [28]. Noteworthily, these two latter compounds are under clinical development. However, the current absence of approved MBL inhibitors and the intrinsic ability of bacteria to develop resistances necessitate further investigation to offer new treatment options.

We are developing MBL inhibitors containing the promising 1,2,4-triazole-3-thione heterocycle as an original ligand for MBL dizinc active sites [36]. Since the first report by Olsen et al. [37] related to the subclass B3 L1 MBL, several random in silico and experimental studies also supported the potential of this heterocycle to inhibit various MBLs of the B1 subclass (i.e. IMP-1 [38], VIM-2 [39] and NDM-1 [40]). In addition, several other crystallographic structures of complexes confirmed that the heterocycle was well adapted to bind into the di-zinc active site of these enzymes. Indeed, in all structures, the heterocycle-thione simultaneously bound to the two Zn ions through two atoms, the heterocyclic nitrogen $N^2$ for Zn1 and the extracyclic sulfur for Zn2 [36,41,42]. Finally, its particular mode of binding might be less efficient toward human metallo-enzymes, which are mainly mono-zinc.

The 1,2,4-triazole-3-thione scaffold offers two modifiable substituents at positions 5 and 4 (Figure 1). In a first study, we explored substitution at position 5, while position 4 was not substituted or only by an amino group [43]. Some compounds showed significant and broad-spectrum inhibition against representative MBLs, but none was able to restore antibiotic activity in MBL-producing resistant bacteria. A second series was that of Schiff base analogues where

an aryl substituent was linked to the 4-amino-heterocycle through a hydrazone-like bond (Figure 1A) [41]. Although the introduction of an aryl substituent at position 4 led to more potent compounds with a broader spectrum of inhibition, no antibiotic potentiation could be achieved against clinical isolates. Poor penetration of the bacterial outer membrane and the potential instability of the hydrazone-like bond to hydrolysis could explain this strong limitation. To solve the instability issue, we first reduced the hydrazone-like bond of selected Schiff base analogues, yielding a third series of compounds (Figure 1B) [44]. Unfortunately, this modification led to less promising compounds. In parallel, we further explored substitution at position 4 by introducing alkyl moieties. A first study identified the high potential of alkanoic chains (Figure 1C) [45]. However, these compounds showed a limited spectrum of activity (no inhibition of NDM-1 and IMP-1) and only modest antibiotic potentiation was observed in microbiological assays. Among these analogues, one possessed an alkanoic chain with a thioether group (compound **1**, Figure 1D). Compound **1** was a potent inhibitor of VIM-type enzymes and showed moderate activity toward NDM-1. Based on these results, we further evaluated the presence of a thioether group in the substituent at position 4 (Figure 1E). We found that the addition of an aryl group at the extremity of the thioether-containing alkyl chain led to potent inhibition of VIM-type enzymes, NDM-1 and IMP-1. In addition, several compounds were able to potentiate meropenem antibacterial activity in clinical multidrug resistant isolates of *K. pneumoniae*. Finally, the resolution of crystallographic structures of complexes with VIM-2 allowed to study the binding mode of these thioether compounds.

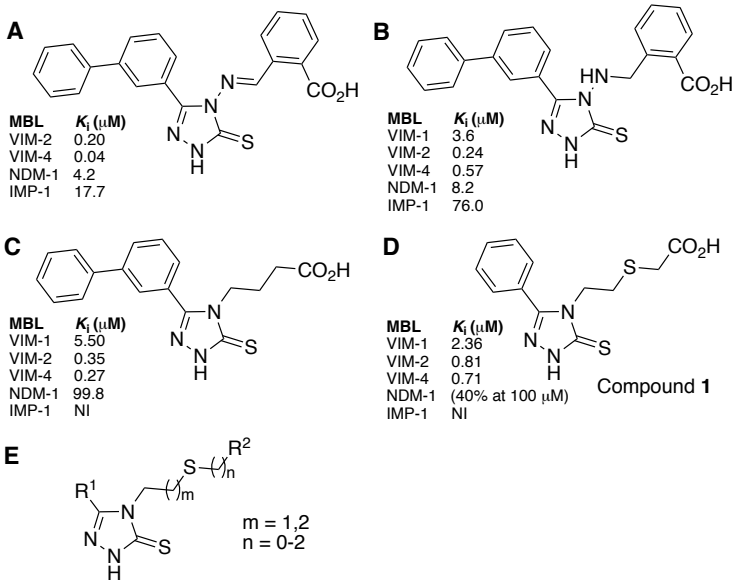


**Figure 1.** Structure of compounds based on the 1,2,4-triazole-3-thione scaffold and their inhibitory potency toward selected MBLs: (A) Schiff base analogue [41]; (B) reduced analogue [44]; (C) 4-alkanoic analogue; [45]; (D) 4-alkanoic analogue with a thioether group, compound **1** [45]; (E) general structure of synthesized compounds containing a thioether group.

## 2. Results and discussion

### *2.1. Synthesis*

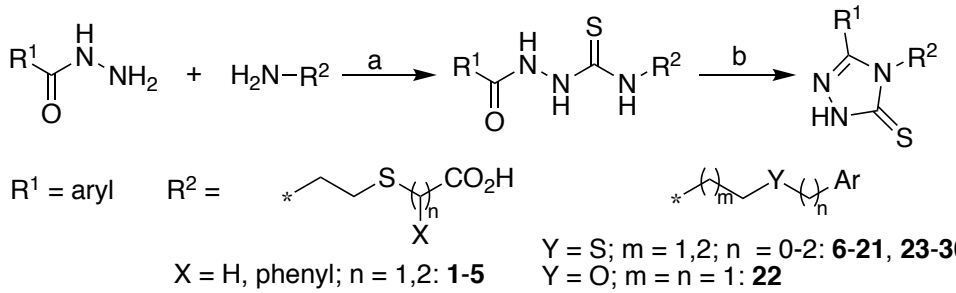


**Scheme 1.** Synthesis of 1,2,4-triazole-3-thione derivatives. *Reagents and conditions: (a) $H_2N$-$R^2$ treated with DPT, $Na_2CO_3$, DMF, 55 °C, 3h; then $R^1$-$CONHNH_2$, DMF, 55 °C, 3h; (b) aqueous KOH or $NaHCO_3$, 100 °C, 3h.*

1,2,4-Triazole-3-thione compounds were prepared from hydrazide and amine precursors in the presence of dipyridylthionocarbonate (DPT) according to Deprez-Poulain et al. [46] and as described [45]. The hydrazides $R^1$-$C(O)NHNH_2$ were first obtained in two steps from the corresponding carboxylic derivative as described in the Supplementary Material part (Scheme S1). The thioether-containing alkylamines $R^2$-$NH_2$ were either commercially available or synthesized as Boc-protected derivatives by alkylation of a thiol with a brominated compound, followed by Boc removal in acidic conditions, as described in the Supplementary Material part (Scheme S2). The ether-containing alkylamine precursor of compound **22** was commercially available. Then, the alkylamines were treated with DPT to yield the intermediate isothiocyanates, which were directly reacted with hydrazides to form the thiosemicarbazide derivatives. Finally, basic treatment induced cyclization toward the expected 1,2,4-triazole-3-thione compounds **1-30** (Scheme 1).

### *2.2 Evaluation of inhibitory potency toward purified MBLs*

Compounds were tested against five representative MBLs, the subclass B1 enzymes VIM-1, VIM-2, VIM-4, NDM-1 and IMP-1. After initial testing at 100 μM, $K_i$ values were measured for compounds exhibiting > 75% inhibition.

The results obtained for a first series of 22 compounds are presented in Table 1. Compound **1** was included for comparison. In this series, all compounds possessed a phenyl ring at position 5 with the exception of compound **5**, which had a *m*-biphenyl group. At position 4, they displayed a diversely *S*-substituted ethyl sulfide group, with the exception of compound **21**, which had a *S*-substituted propyl sulfide group and of compound **22** where the sulfur was

replaced by an oxygen. Compared to compound **1**, compound **2** possessed a one-methylene longer chain with a *S*-propanoic substituent and a quite similar activity profile, although it also significantly inhibited IMP-1. Adding a phenyl ring at the α-position of the carboxyl group of compounds **1** and **2** yielded compounds **3** and **4**, respectively. Whereas compound **3** showed similar activities as **1**, the presence of the aromatic moiety was highly beneficial for compound **4**. Indeed, this compound showed submicromolar $K_i$ values against both VIM-type enzymes, was a micromolar inhibitor of NDM-1 and significantly inhibited IMP-1. As we previously found that a *m*-biphenyl substituent at position 5 was favourable to inhibition, we synthesized the corresponding analogue of **4**, i.e. compound **5**. However, although **5** was also a potent inhibitor of VIM-type enzymes, this modification did not improve the activity and was slightly detrimental to NDM-1 and IMP-1 inhibition.

Because compounds **3** and **4** possessed a chiral center and an α-branched alkanoic chain that could complicate further development of this series, we removed the carboxylic group to check its importance in MBL inhibition, giving compounds **6** and **13**, respectively. In fact, this modification was favourable for compound **6** as, in addition to be a slightly better VIM inhibitor, it also inhibited NDM-1 and IMP-1 with $K_i$ values around 20 μM. Compound **13** showed similar activities against all enzymes as **6**. These results indicated that the carboxylic group was not essential in this series.

Based on these data, we prepared a small series of **6** analogues where the phenyl group of the 4-substituent was diversely substituted (compounds **7**-**12**). All molecules were potent inhibitors of both VIM-type enzymes as **6**, showing $K_i$ values in the low micromolar to submicromolar range. In addition, most compounds (i.e. **7**-**11**) were also moderate to good inhibitors of NDM-1 and IMP-1. Compound **11** showed one of the broadest spectrum of activity in this series.

As the separation of the phenyl ring from the sulfur atom by one (**6**) or two (**13**) methylenes gave potent MBL inhibitors, we assessed if its direct attachment was also tolerated (i.e. compound **14**). It was indeed the case as compound **14** showed an inhibition profile similar to that of **11**. Therefore, we prepared a short series of compounds (**15**-**20**) with various aryl and heteroaryl moieties directly attached to the sulfur. Unfortunately, these modifications were generally detrimental for the inhibitory activity, excepted **15** (aniline) with similar profile as **14**, and **16** (naphtha-1-yl), which however only inhibited VIM-type enzymes. Increasing the distance between the triazole ring and the sulfur from ethyl to propyl gave compound **21**, which was a rather potent inhibitor of VIM-type enzymes although with a lower potency when compared to that of the shorter **14** and compound **6**, which possessed a 4-substituent of same

size and composition but where the sulfur was shifted by one atom. In addition, **21** only moderately inhibited NDM-1 and IMP-1. This result indicated the importance of the sulfur atom and of its position for MBL inhibition. It was confirmed by replacing the sulfur atom of compound **6** by an oxygen (i.e. compound **22**). Indeed, the ether **22** showed a very similar activity profile as **21**, and therefore was a less potent inhibitor of both enzymes compared to **6**. It is noteworthy that the thioether moiety exhibits an angle close to 90°, while that of an ether is close to 110°. This difference, which should have an impact in substituent positioning may at least partially explain the difference in activity between the analogues **6** and **22**.

**Table 1.** Inhibitory activity of 1,2,4-triazole-3-thione analogues **1**-**22** against various MBLs.[a]

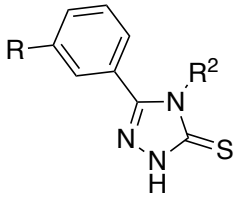


| Cpd | Structure | $K_i$ (μM) or (% inhibition at 100 μM) | | | | |
|---|---|---|---|---|---|---|
| | $R^2$ | VIM-1 | VIM-2 | VIM-4 | NDM-1 | IMP-1 |
| **1**[b] | 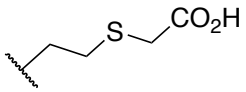 | 2.36 ± 0.14 | 0.81 ± 0.04 | 0.71 ± 0.06 | (40%) | NI |
| **2** | 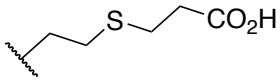 | 1.99 ± 0.18 | 1.91 ± 0.09 | 1.98 ± 0.12 | (59%) | (67%) |
| **3** | 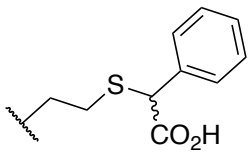 | 1.65 ± 0.16 | 0.19 ± 0.01 | 0.21 ± 0.02 | (40%) | (30%) |
| **4** | 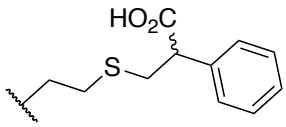 | 0.48 ± 0.06 | 0.60 ± 0.04 | 0.22 ± 0.02 | 6.0 ± 1.0 | 35.0 ± 11.0 |
| **5**[a] | | 1.39 ± 0.13 | 0.37 ± 0.02 | 0.21 ± 0.01 | 20.3 ± 1.7 | (56%) |
| **6** | 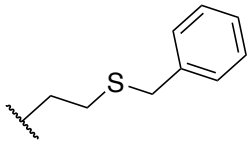 | 0.21 ± 0.02 | 0.24 ± 0.36 | 0.31 ± 0.07 | 22.3 ± 1.9 | 19.6 ± 2.5 |
| **7** | 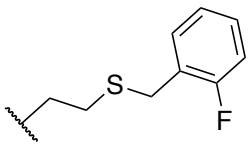 | 0.59 ± 0.03 | 0.28 ± 0.01 | 0.32 ± 0.02 | 11.9 ± 0.4 | 12.1 ± 1.0 |

| | | | | | | |
|---|---|---|---|---|---|---|
| **8** | 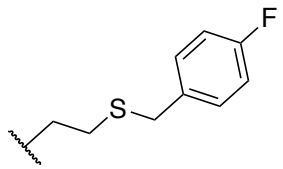 | 2.22 ± 0.16 | 0.83 ± 0.04 | 1.11 ± 0.04 | 15.1 ± 2.9 | 9.66 ± 1.43 |
| **9** | 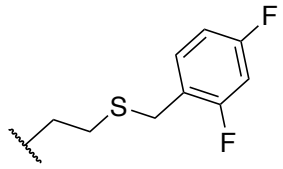 | 1.33 ± 0.10 | 0.94 ± 0.06 | 1.18 ± 0.03 | 12.0 ± 1.8 | 8.67 ± 1.69 |
| **10** | 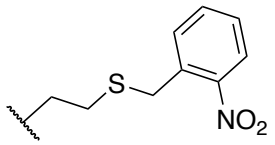 | 0.480 ± 0.004 | 0.57 ± 0.03 | 0.56 ± 0.07 | 13.2 ±1.1 | (72%) 19[c] |
| **11** | 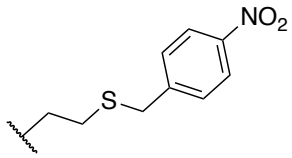 | 0.43 ± 0.02 | 1.29 ± 0.17 | 0.88 ± 0.03 | 11.1 ± 2.1 | 3.63 ± 0.33 |
| **12** | 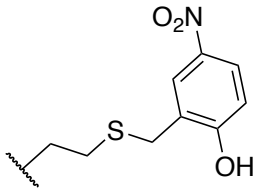 | 0.58 ± 0.03 | 0.21 ± 0.01 | 0.25 ± 0.02 | 11.9 ± 1.2 | (62%) |
| **13** | 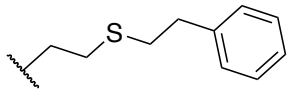 | 0.46 ± 0.02 | 1.76 ± 0.11 | 0.43 ± 0.03 | 21.1 ± 2.9 | 17.7 ± 2.4 |
| **14** | 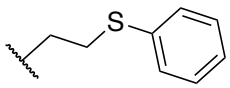 | 1.26 ± 0.07 | 1.57 ± 0.13 | 0.54 ± 0.07 | 11.0 ± 2.0 | 3.35 ± 0.53 |
| **15** | 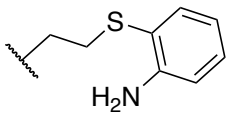 | 0.47 ± 0.04 | 1.15 ± 0.09 | 0.41 ± 0.02 | 16.3 ± 2.4 | 22.2 ± 3.2 |
| **16** | 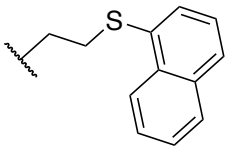 | 0.48 ± 0.05 | 1.00 ± 0.11 | 0.25 ± 0.04 | NI | NI |
| **17** | 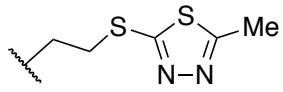 | 2.17 ± 0.15 | (56%) | 2.95 ± 0.22 | NI | NI |
| **18** | 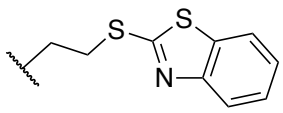 | NI | (30%) | (44%) | NI | (47%) |

| | | | | | | |
|---|---|---|---|---|---|---|
| **19** | 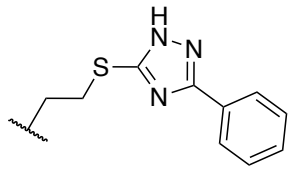 | NI | (44%) | (52%) | NI | (32%) |
| **20** | 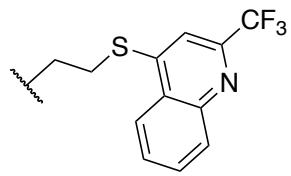 | (37%) | NI | NI | 12.9 ± 2.2 | NI |
| **21** | 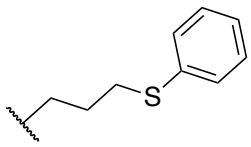 | 2.98 ± 0.25 | 1.35 ± 0.23 | 4.85 ± 0.58 | (42%) | (46%) |
| **22** | 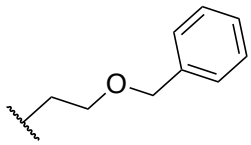 | 1.02 ± 0.10 | 3.16 ± 0.10 | 2.06 ±0.19 | (33%) | (42%) |

[a]For all compounds, R = H, excepted compound **5** for which R = phenyl. All kinetic assays were performed in triplicate. NI: no inhibition (< 30% inhibition at 100 μM). [b]From reference [45]. [c]Apparent $K_i$ value, not determined due to non linear $v_0/v_i$ vs [I] plot.

Overall, the presence of a thioether group in the 4-alkyl chain and a phenyl ring at its extremity was quite favourable to potent and broad-spectrum inhibition of MBLs, while a carboxylic group could be spared. The position of the sulfur relative to the triazole moiety was critical for activity, while its replacement by an oxygen was deleterious.

Based on the results obtained with compounds possessing a phenyl group at the 5-position (with the exception of compound **5**), we prepared a series of compounds derived from compound **6**, with an ethyl benzyl sulfide substituent and a variable aryl group at positions 4 and 5, respectively (Table 2). The aryl groups were chosen according to inhibition data obtained with our previously reported series of 1,2,4-triazole-3-thione-based MBL inhibitors [41,44,45].

Compounds **23** (o-toluyl), **24** (2-hydroxy-5-methoxy) and **25** (1-methyl-pyrrol-2-yl), were potent inhibitors of both VIM-type enzymes with $K_i$ values in the submicromolar range. NDM-1 and IMP-1 were also significantly inhibited by these compounds, although less potently in the case of **24**. However, substituting the phenyl ring at position 5 did not improve the inhibitory profile compared to **6**. Based on its potency and broad spectrum of inhibition, compound **25** was subjected to a Dixon plot analysis (Figure 2) with the VIM-1 MBL. The data obtained were compatible with a competitive mechanism of inhibition and confirmed the submicromolar $K_i$ value (0.20 ± 0.02 μM).

**Table 2.** Inhibitory activity of 1,2,4-triazole-3-thione analogues **23-30** with $R^2$ = ethyl benzyl sulfide against various MBLs.[a]

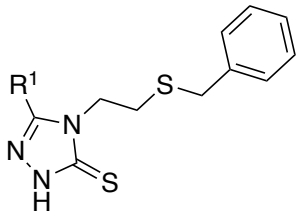


| Cpd | Structure | $K_i$ (μM) or (% inhibition at 100 μM) | | | | |
|---|---|---|---|---|---|---|
| | **$R^1$** | **VIM-1** | **VIM-2** | **VIM-4** | **NDM-1** | **IMP-1** |
| **23** | 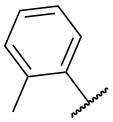 | 0.40 ± 0.04 | 0.80 ± 0.09 | 0.50 ± 0.04 | 13.0 ± 1.0 | 44.0 ± 8.0 |
| **24** | 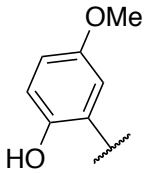 | 0.18 ± 0.02 | 1.65 ± 0.16 | 0.60 ± 0.10 | (46%) | (63%) |
| **25** | 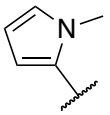 | 0.23 ± 0.01 | 0.34 ± 0.01 | 0.25 ± 0.01 | (75%) 28[b] | 9.04 ± 1.53 |
| **26** | 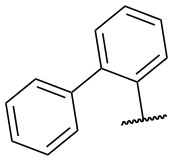 | ND | NI | ND | NI | (35%) |
| **27** | 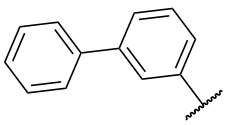 | NI[c] | NI[c] | 0.89 ± 0.22 | NI | (21%)[c] |
| **28** | 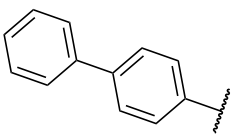 | NI[c] | NI | NI[c] | NI | (60%) |
| **29** | 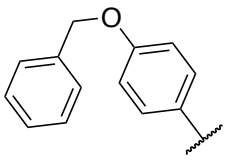 | 2.24 ± 0.58 | NI | 1.04 ± 0.18 | NI | (60%) |
| **30** | 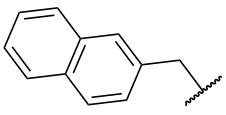 | NI[c] | NI | (23%)[c] | NI | (70%) |

[a]All kinetic assays were performed in triplicate. NI: no inhibition (< 30% inhibition at 100 µM or < 15% inhibition at 25 µM). ND: not determined. [b]Approximate $K_i$ value, not determined due to non-linear $v_0/v_i$ vs [I] plot. [c]Tested at 25 µM due to poor solubility in HEPES 50 mM.

We also prepared compounds with two aromatic groups at position 5 because these substituents were previously found to be highly favourable to MBL inhibition [41,44,45]. They displayed an *ortho*- (**26**), *meta*- (**27**), or *para*-biphenyl (**28**) group, a *p*-benzyloxyphenyl (**29**), or a naphth-2-yl-methyl (**30**) group. Unfortunately, the inhibitory data obtained with these compounds were quite disappointing as none inhibited VIM-2 and NDM-1 and they were generally only modest or not inhibitors of the other tested MBLs. In particular, compound **27**, which possesses a *m*-biphenyl group previously shown to be the most favourable substituent at this position, only inhibited VIM-4. In addition, some of these compounds (**27**,**28**,**30**) suffered of low solubility.

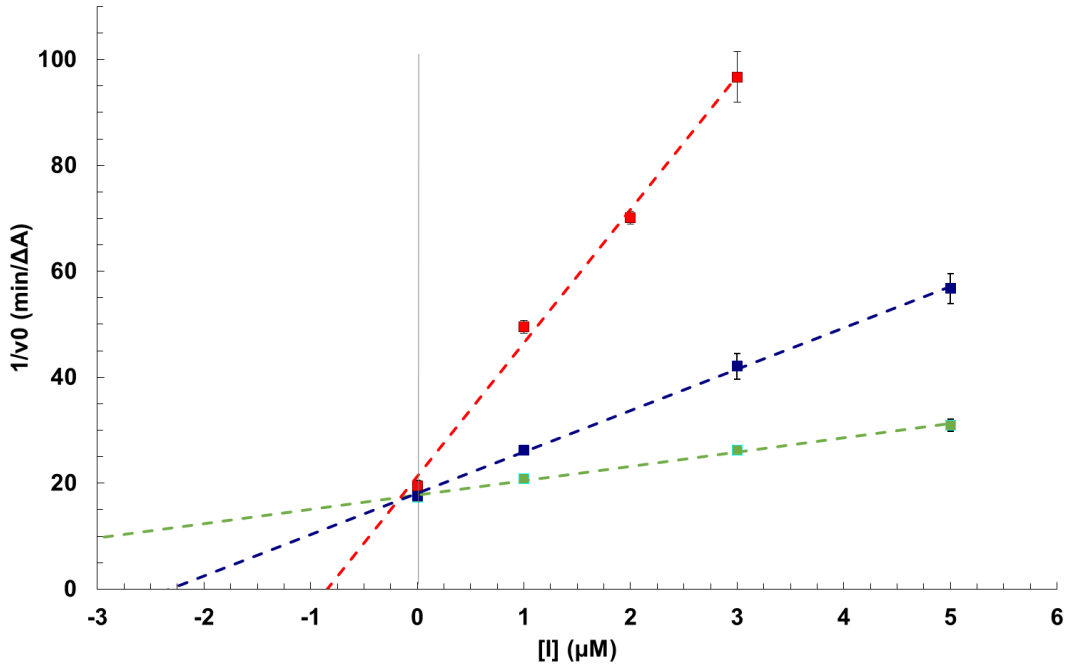


**Figure 2.** Dixon plot analysis of VIM-1 inhibition by compound **25**. Imipenem was used as the reporter substrate (VIM-2 $K_m$ value, 9 µM). Inhibition data were obtained at 100, 300 and 1000 µM of substrate (red, blue and green, respectively) and in the presence of inhibitor concentrations ranging 1-5 µM.

### *2.3 Crystal structures of the complexes between VIM-2 and compounds **8**, **10** and **14***

The structure of VIM-2 in complex with three inhibitors, compounds **8**, **10**, and **14**, was determined at resolutions ranging from 1.80 to 1.92 Å (Table S1).

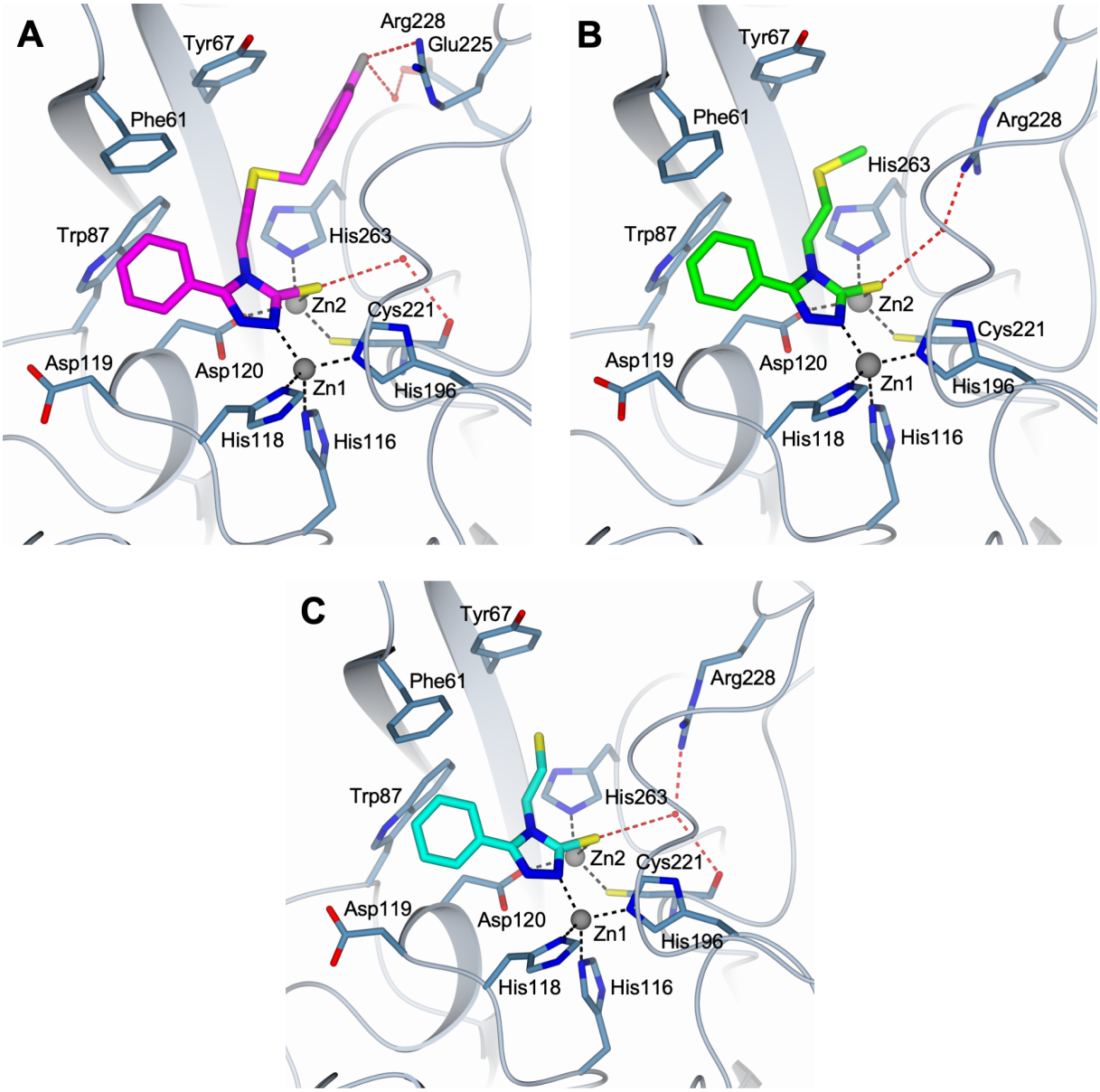


**Figure 3.** Active-site view of VIM-2 (steel blue cartoon and carbon atoms; residues in sticks) in complex with A) **8** (in sticks, magenta carbons, PDB code 7OVF), B) **10** (in stick, green carbons, PDB code 7OVE), C) **14** (in stick, cyan carbons, PDB code 7OVH). In all figures, Zn ions and water molecules are displayed as grey and red spheres (arbitrary radius), respectively. Hydrogen and coordination bonds are represented as red and black dashed lines. Oxygen atoms are colored red, nitrogen blue, sulfur yellow, and fluorine grey.

The binding mode of the shared 1,2,4-triazole-3-thione core of the compounds is highly conserved, retaining the same interactions within the enzyme cavity in all complexes (Figures 2 and S1). The nitrogen 2 completes the Zn1 coordination, whereas the thione coordinates Zn2. The latter molecular function is further stabilized by water-mediated interactions with either Cys121 backbone carbonyl (compound **8**, Figure 3A) or Arg228 guanidinium (compound **10**, Figure 3B) or both (compound **14**, Figure 3C). The phenyl ring at position 5 forms T-shaped interaction with Phe61 and van der Waals interactions with Trp87 and Asp119 (aliphatic portion

of the side chain) (Figures 3 and S1). The shared ethyl sulfide group is accommodated in the hydrophobic region lined by Phe61, Tyr67, Trp87, and His263. In the complex with **8**, the *p*-fluorine phenyl forms a distorted T-shaped interaction with the aromatic system of Tyr67. The *p*-fluorine forms also hydrogen bonds with the guanidinium nitrogen of Arg228 and with a water molecule, further H-bonded to Glu225 (Figure 3A). The interaction with Arg228 involves a different positioning of the residue side-chain compared to its orientation in complexes with compounds **10** and **14**. An additional halogen bond is formed by the same fluorine with the backbone carbonyl of Asp63 belonging to a symmetry-related VIM-2 molecule (interaction not shown in Figure 3A; since VIM-2 is monomeric this additional interaction is due to the crystal packing). On the other hand, in the complexes with **10** and **14** the terminal phenyl and *o*-nitrophenyl moieties, respectively, are characterized by positional disorder (reasonably due to ring rotation) and thus excluded from our models (Figures 3B-C and S1B-C).

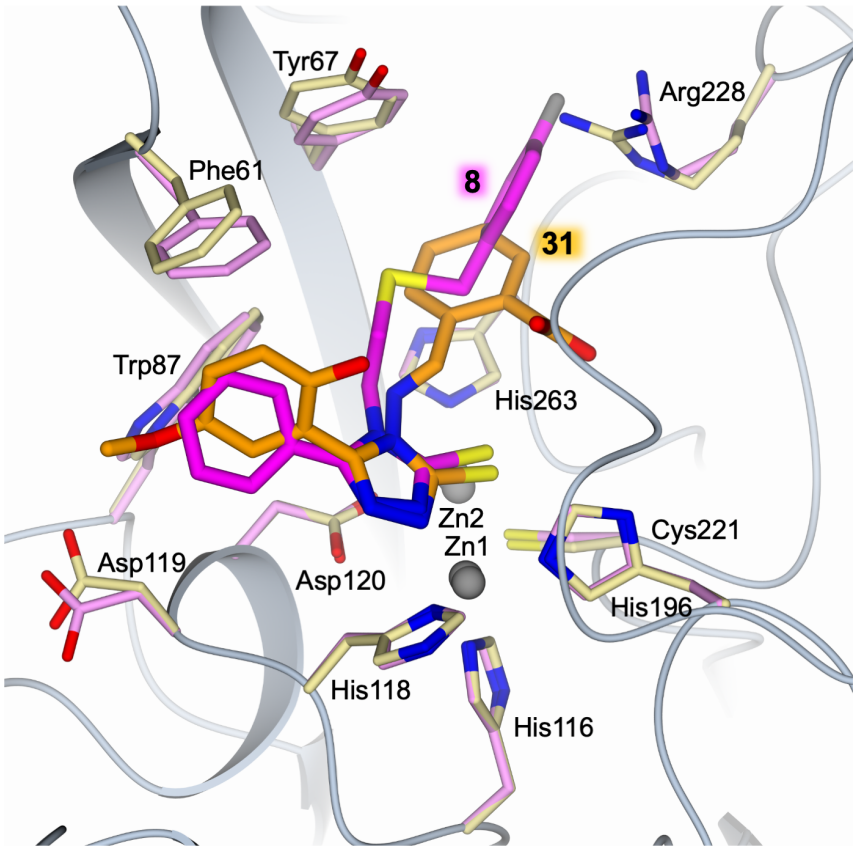


**Figure 4.** Active site view of the superimposition between the structures of VIM-2 (steel blue cartoon and carbons, residues in sticks) in complex with **8** (in sticks, magenta carbons; residues in sticks, light magenta carbons) and the Schiff base **31** (PDB code 6YRP, numbering from reference [41]; **31** and residues in sticks, orange and light orange carbons, respectively).

We previously reported the characterization of VIM-2 in complex with a 4-amino-1,2,4-triazole-3-thione-derived Schiff base (PDB code 6YRP, compound **31** in reference [41]). The

comparison with the binding modes of the 1,2,4-triazole-3-thione compounds **8**, **10**, and **14** highlights the conserved interactions formed by the shared triazole-thione core of the inhibitors, involved in the coordination of both Zn1 and Zn2 ions inside the cavity (Figure 4). Analogous interactions are also formed by the shared 5-phenyl moiety of the inhibitors, accommodated in the pocket lined by Phe61, Trp87, and Asp119. At the opposite side of the cavity, the variable molecular functions introduced at position 4 determine peculiar interactions in this area. In compounds **8**, **10**, and **14**, the increased length of the ethyl sulfide group allows to explore a different portion of the active site cavity, lined by Tyr67, Arg228, and His263 (Figure 4).

### *2.4. Equilibrium dialysis and native state electrospray ionization mass spectrometry (native MS)*

We further evaluated the mechanism of inhibition of this series of compounds by studying the effect of compound **6** on the metal content of VIM-2 and NDM-1 using equilibrium dialysis followed by metal analysis with atomic absorption spectroscopy [23,47]. At concentrations up to 48 μM, the compound did not remove Zn(II) from either VIM-2 or NDM-1 (Figure S3), suggesting the formation of a ternary complex between the inhibitor and both MBLs in agreement with previous and here presented crystallographic data [36,41,42].

Native MS is an efficient technique used to probe the mechanism of inhibition at low enzyme/inhibitor concentrations. The experiment was performed using 10 μM NDM-1 and 5 equivalents of compound **6**. The native MS of the MBL with **6** showed two main peaks: a dominant +8 peak at 3,174 m/z, and a non-dominant +8 peak at 3,214 m/z, corresponding to the mass of two Zn(II) bound NDM-1 (25,385 Da) and to that of two Zn(II) bound NDM-1 with one equivalent of compound **6** (25,712 Da), respectively. This result further supports the formation of a ternary complex with NDM-1 (Figure S4).

### *2.5.* In vitro *antibacterial synergistic activity*

Considering the significant potency of several compounds towards all tested MBLs and in particular on VIM-type enzymes, their potential synergistic activity was tested using the broth microdilution method on several MBL-producing multidrug-resistant clinical isolates. First, it was assessed that (a) none of the compounds showed any direct or intrinsic antibacterial activity (MIC > 512 μg/mL) and that (b) the stability of meropenem was not affected by the presence of selected inhibitor for up to 4 hours at 35 °C (measured in both 50 mM HEPES buffer, pH 7.5, and in Mueller-Hinton broth, by following the absorbance at 300 nm, as previously

described; data not shown) [48,49]. Tested at a fixed concentration of 32 μg/mL (essentially to generate data comparable to that of previous series [41,43-45]), most compounds were able to reduce the MIC of meropenem on *K. pneumoniae* isolates producing VIM-1 or VIM-4 (Table 3). Indeed, in these conditions, several showed up to a remarkable 16-fold potentiation of meropenem (compounds **2**, **7**, **9**-**14**, **21** and **25**). In particular, compound **14** displayed a similar potentiation against both isolates. There was no clear relationship between inhibitory potencies and synergistic antibacterial activities, suggesting that structural modifications would differently impact on enzyme inhibition and the ability of the compound to readily accumulate in the periplasmic space through rapid diffusion across the outer membrane. In particular, the potent VIM inhibitors **16** and **27** were unable to potentiate meropenem in these experiments. To assess whether the compounds would show a true synergistic activity (rather than an additive effect), a chequerboard analysis was carried out with two potent inhibitors of VIM-4, compounds **13** and **25,** and meropenem (the VIM-4-producing *K. pneumoniae* VA-416/02 strain was used) (Table S2, Figure S2). The inhibitors showed a dose-dependent effect. Overall, compound **25** showed a better activity as it was able to restore a meropenem MIC of 2 μg/mL (16-fold potentiation) already at 8 microg/mL, while compound **13** only achieved a two-fold potentiation at this concentration. Nonetheless, the resulting average FIC index values were 0.459 and 0.347, for compounds **13** and **25** respectively, i.e. below 0.5 in both cases, indicating that the MBL inhibitors act synergistically with meropenem to potentiate its activity [50,51]. Furthermore, since compound **25** exhibited among the most potent *in vitro* enzyme inhibition and meropenem potentiation on VIM-producing clinical isolates, the bactericidal activity of the combination meropenem:**25** was investigated with time-kill curves. This compound alone, at 32 μg/mL, did not minimally affect bacterial growth. However, in combination with 2 μg/mL meropenem (equivalent to the susceptibility breakpoint), **25** proved able to restore the bactericidal activity of the antibiotic (reduction of $>3\log_{10}$ viable bacteria) against the VIM-4-producing *K. pneumoniae* isolate VA-416/02 (starting inoculum, $5 \times 10^6$ CFU/mL), within 3 hours (bacterial count, $1.1 \times 10^3$ CFU/mL; reduction fold, ≈ 4,500).

A few compounds were tested on the same clinical isolates in the presence of other carbapenems (i.e. imipenem (IPM), doripenem (DOR) and ertapenem (ETP)) (Table S3). Compared to meropenem, some compounds also showed similar potentiating activity with IPM. This activity was lower with DOR and absent with ETP. In the latter case, this result might be explained by the lower MIC values of ETP (8- to 16-fold) compared to the other carbapenems. In this assay, compound **7** showed the strongest activity toward both clinical isolates and for both IPM and MEM. A similar experiment was performed with compound **9** ($K_i$ = 12.0 ± 1.8 μM against

NDM-1) on two NDM-1-and NDM-4-producing clinical isolates (Table S4). Compound **9** showed modest potentiating activity in the presence of DOR only (4-fold reduction of its MIC) with the NDM-1-producing isolate.

**Table 3.** Antibacterial synergistic activity of compounds on VIM-1-and VIM-4-producing *K. pneumoniae* clinical isolates with meropenem determined by the broth microdilution method.

| **Cpd** (32 μg/mL) | **Meropenem MIC[a] (μg/mL) and $K_i$ (μM) values of selected inhibitors** | | | |
|---|---|---|---|---|
| | *K. pneumoniae* 7023 ($bla_{VIM\text{-}1}^{+}$) | | *K. pneumoniae* VA 416/02 ($bla_{VIM\text{-}4}^{+}$) | |
| | MEM MIC | $K_i$ (VIM-1)[b] | MEM MIC | $K_i$ (VIM-4)[b] |
| None | 16 | - | 16 | - |
| **1**[c] | 2 | 2.36 ± 0.14 | 4 | 0.71 ± 0.06 |
| **2** | 2 | 1.99 ± 0.18 | 1 | 1.98 ± 0.12 |
| **3** | 4 | 1.65 ± 0.16 | 2 | 0.21 ± 0.02 |
| **4** | 2 | 0.48 ± 0.06 | 4 | 0.22 ± 0.02 |
| **5** | 4 | 1.39 ± 0.13 | 2 | 0.21 ± 0.01 |
| **6** | 2 | 0.21 ± 0.02 | 4 | 0.31 ± 0.07 |
| **7** | 1 | 0.59 ± 0.03 | 2 | 0.32 ± 0.02 |
| **8** | 8 | 2.22 ± 0.16 | 2 | 1.11 ± 0.04 |
| **9** | 2 | 1.33 ± 0.10 | 1 | 1.18 ± 0.03 |
| **10** | 2 | 0.480 ± 0.004 | 1 | 0.56 ± 0.07 |
| **11** | 2 | 0.43 ± 0.02 | 1 | 0.88 ± 0.03 |
| **12** | 1 | 0.58 ± 0.03 | 4 | 0.25 ± 0.02 |
| **13** | 2 | 0.46 ± 0.02 | 1 | 0.43 ± 0.03 |
| **14** | 1 | 1.26 ± 0.07 | 1 | 0.54 ± 0.07 |
| **15** | 4 | 0.47 ± 0.04 | 2 | 0.41 ± 0.02 |
| **16** | 8 | 0.48 ± 0.05 | 16 | 0.25 ± 0.04 |
| **17** | 2 | 2.17 ± 0.15 | 2 | 2.95 ± 0.22 |
| **21** | 2 | 2.98 ± 0.25 | 1 | 4.85 ± 0.58 |
| **22** | 4 | 1.02 ± 0.10 | 2 | 2.06 ± 0.19 |
| **23** | 4 | 0.40 ± 0.04 | 2 | 0.50 ± 0.04 |
| **24** | 2 | 0.18 ± 0.02 | 2 | 0.60 ± 0.10 |

| | | | | |
|---|---|---|---|---|
| **25** | 2 | 0.23 ± 0.01 | 1 | 0.25 ± 0.01 |
| **27** | 16 | NI | 16 | 0.89 ± 0.22 |

[a]MEM, meropenem. [b]From Tables 1 and 2. [c]Data from reference [45]. NI: no inhibition.

Finally, a few compounds were also evaluated on a NDM-1-producing *E. coli* clinical isolate (SI-004M) in the presence of meropenem but none showed potentiation activity (Table S5). This result might be due to their 10- to 100-fold lower inhibitory potency against NDM-1 compared to VIM-1 and VIM-4 and/or to insufficient accumulation into the periplasmic space. To check the latter hypothesis, a sub-inhibitory concentration of colistin (not affecting MIC values alone), a polymyxin antibiotic with known membrane permeabilizing properties [52], was added to the medium. In these conditions, several compounds (**6**, **9**, **13**) showed synergistic activity (Table S5). In particular, compound **13** induced a remarkable 128-fold potentiation of meropenem. However, the reasons why other compounds with higher inhibitory potency were poorly active in microbiological assays are not clear.

Overall, compounds of the present series could restore the susceptibility of MBL-producing clinical isolates to a carbapenem with higher efficiency compared to the recently published alkanoic series, supporting the interest for further medicinal chemistry efforts.

### *2.6. Cytotoxicity assays on mammalian cells*

The potential cytotoxic activity of several compounds was evaluated using a membrane integrity assay (CytoTox 96®, Non-Radioactive Cytotoxicity Assay, Promega). They were tested for their ability to induce the lysis of HeLa cells at concentrations up to 250 μM (Table 4). Half of the tested compounds (**4**, **12**, **25**) showed $IC_{50}$ values > 250 μM, indicating that they do not induce cell lysis. Others (i.e. **6**, **7**, **23**) displayed moderate toxicity but with $IC_{50}$ values greater than 100 μM.

A further evaluation of their potential cytotoxicity was performed using the RealTime-Glo MT Viability Assay, which substantially confirmed these results, showing no additional cytotoxicity upon exposure of HeLa cells to the compound (at the $IC_{50}$ concentration) for up to 48 hours. Additional cytotoxicity assays were performed using the A549 human cell line (adenocarcinomic human alveolar basal epithelial cells) on selected compounds (**12** and **25**). Although compound **12** showed a slightly higher cytotoxic activity after exposure to the compound for up to 48 h towards this cell line ($IC_{50}$, 125 μM), compound **25** did not inhibit cell viability and proliferation ($IC_{50}$, >250 μM).

Finally, the toxicity of selected compounds (**6**, **7**, **12**, **25**) was also assessed on normal human cells, i.e. Peripheral Blood Mononucleated Cells (PBMC) from four donors (Table S6). Compound **12** showed no toxicity after 24h with $IC_{50}$ values above 500 μM for all donors while **7** was the most toxic with $IC_{50}$ values comprised between 175 and 377 μM. Compounds **6** and **25** were not toxic toward the PBMC of two donors ($IC_{50}$ > 500 μM) but lower $IC_{50}$ values (about 200-300 μM) were measured for the two other samples. Overall, these compounds showed no or only moderate toxicity in this assay.

Tested in both three assays, **25** appeared to be one of the best compounds in terms of enzyme inhibition, antibiotic potentiation and selectivity.

**Table 4.** Cytotoxic activity against HeLa cells.

| Cpd | HeLa cells $IC_{50}$ (μM) | Cpd | HeLa cells $IC_{50}$ (μM) |
|---|---|---|---|
| **4** | > 250 | **12** | > 250 |
| **6** | 152 ± 16 | **23** | 121 ± 10 |
| **7** | 165 ± 29 | **25** | > 250 |

*2.7. Selectivity toward human glyoxalase II*

The potential inhibitory activity of compound **6** on human glyoxalase II, a di-zinc metallo-hydrolase belonging to the MBL superfamily was determined. It could inhibit human glyoxalase II but moderately with an $IC_{50}$ value of 52 μM, showing clear selectivity in favour of MBL enzymes.

## 3. Conclusions

Introducing an ethyl alkyl sulfide chain at position 4 of 5-substituted 1,2,4-triazole-3-thione derivatives yielded potent broad-spectrum inhibitors of clinically relevant subclass B1 MBLs with $K_i$ values in the micromolar to submicromolar range against three VIM-type MBLs, NDM-1 and IMP-1. Kinetic and structural data largely support a competitive mechanism of inhibition. Compared to the previously reported alkanoic series [45], these results represented significant progress as VIM-1, NDM-1 and IMP-1 were not or only poorly sensitive to this older series of compounds. The extended inhibition spectrum now including the three MBL enzyme subgroups was largely relying on the introduction of a phenyl moiety. However, the better activity against VIM-1 was also due to the presence of the sulfur atom. Indeed, the carba (i.e.

sulfur replaced by $CH_2$) analogues of compounds **1** and **2** were around 6- and 2-fold less potent against this enzyme, respectively [35]. Furthermore, it was possible to remove the carboxylic group present in most best compounds identified in previous series [41,44,45]. It is an interesting result as this ionizable group is generally considered to limit membrane permeation. Replacing the sulfur of compound **6** by an oxygen (**22**) yielded less potent compounds, showing again the favorable role of this heteroatom. In addition, its position relative to the triazole ring looked critical. The role played by the sulfur might at least partially come from the nearly right angle of the thioether moiety compared to the 110° angle of an ether or the corresponding alkyl group.

Three crystal structures of VIM-2 complexes were obtained and showed the same binding mode of the triazole-thione moiety in the di-zinc active site of the enzyme, when compared to previously reported structures. The positions of compounds **8**, **10** and **14** are largely superimposable, including the flexible thioether chain lying on a hydrophobic region of the VIM-2 binding site, although the phenyl ring present at its extremity was not visible in the case of **10** and **14**. Interestingly, the same phenyl ring in compound **8** showed a stable position, thanks to its fluorine substituent, which establishes stabilizing interactions, including with an arginine guanidinium group. This result will be taken into account in the design of future molecules.

Microbiological assays showed that many compounds of this series were able to significantly potentiate the activity of meropenem toward VIM-producing clinical isolates of *K. pneumoniae* with a reduction of the antibiotic MIC up to 16-fold. Compared to previous series [41,44,45], these inhibitors showed a better ability to accumulate in the periplasm at concentrations compatible with efficient MBL inhibition in the bacterial cell. These favourable results might be due to their higher hydrophobicity compared to best inhibitors of previous series, which often contained a carboxylic group.

Finally, cytotoxicity experiments and the study of a potential off-target (i.e. glyoxalase II) afforded quite favourable results.

These promising results support the interest to continue the development of 1,2,4-triazole-3-thione-based compounds. Further modification at position 4 is ongoing to obtain compounds characterized with both better inhibitory activity against NDM-1 and better synergistic antibacterial activity.

## 4. Experiment section

*4.1. Chemistry section*

The compound synthesis was adapted from Deprez-Poulain et al. [46] and performed as previously described [45]. General procedures for the preparation of 1,2,4-triazole-3- thiones as well as of the hydrazide and amine precursors are presented in the Supplementary Material section. The physico-chemical properties of final compounds are also described in the Supplementary Material section. Their purity was determined to be ≥95% by $^{1}$H NMR and reverse phase HPLC.

*4.2. Biology section*

*4.2.1. Metallo-β-Lactamase inhibition assays*

*4.2.1.1 VIM-type enzymes, NDM-1 and IMP-1*

The inhibition potency of the compounds has been assessed with a reporter substrate method and specifically by measuring the rate of hydrolysis of 150 μM imipenem or 150 μM meropenem at 30 °C in 50 mM HEPES buffer (pH 7.5) in the absence and presence of several concentrations of the inhibitor (final concentration, 0.5–1,000 μM). Final DMSO concentration in the assays was 0.5%.

The reaction rate was measured as the variation of absorbance observed upon substrate hydrolysis in a UV-Vis spectrophotometer or microplate reader at a wavelength of 300 nm (imipenem, meropenem) and in the presence of a purified MBL enzyme (VIM-1, VIM-2, VIM-4, NDM-1, IMP-1) at a final concentration ranging from 1-70 nM). In some cases (as indicated in Tables), a 10 min pre-incubation of enzyme and compound was done.

The inhibition constants ($K_i$) were determined on the basis of a model of competitive inhibition by analyzing the dependence of the ratio $v_0/v_i$ ($v_0$, hydrolysis velocity in the absence of inhibitor; $v_i$, hydrolysis velocity in the presence of inhibitor) as a function of [I] as already described [53]. The slope of the plot of $v_0/v_i$ *vs* [I], which corresponds to $K_m^S/(K_m^S + [S])K_i$ (where $K_m^S$ is the $K_m$ value of the reporter substrate and [S] its concentration in the reaction mixture) and allowed the calculation of the $K_i$ value. Alternatively, a Dixon plot analysis was carried out by measuring the initial hydrolysis rates in the presence of variable concentrations of inhibitor and substrate. This allowed $K_i$ values to be determined and supported the hypothesis that the various compounds behaved as competitive inhibitors of the various tested enzymes. All assays were performed in triplicate.

*4.2.2. Microbiological assays*

The minimum inhibitory concentrations (MICs) of carbapenems (meropenem, imipenem, ertapenem and doripenem) were determined in triplicate using Mueller-Hinton broth (MHB) and a bacterial inoculum of $5 \times 10^4$ CFU/well, as recommended by the CLSI [54], in both the absence and presence of a fixed concentration (32 μg/mL) of an inhibitor. The antibiotics and compounds were diluted from a stock solution (1.2 mg/mL meropenem in sterile milliQ water; 3.2 mg/mL inhibitor in DMSO) in MHB. For assessing the activity of the combination, the inhibitor was added at 32 μg/mL to the wells immediately prior to the addition of the antibiotic diluted in MHB containing 32 μg/mL inhibitor and the two-fold serial dilutions. Multidrug resistant VIM-1- or VIM-4-producing *K. pneumoniae* clinical isolates present in our collection (7023 and VA-416/02, respectively) [55,56] were used and added extemporaneously to each well, prior to incubation of the plates at 35 °C for 24 h. Negative and positive growth controls were also prepared. The residual concentration of DMSO in the assay did not exceed one percent. Results were read following visual inspection of the plates. A multidrug resistant NDM-1-producing *E. coli* clinical isolate (SI-004M) was also used. In this case, the experiment was also performed in the absence and the presence of a sub-inhibitory concentration of colistin (0.12 μg/mL) [45]. Chequerboard analysis was carried out with selected inhibitors and meropenem using the VIM-4-producing *K. pneumoniae* clinical isolate VA-416/02, as previously described [50,51]. Time-dependent bacterial killing of meropenem/inhibitor combination was investigated using established methods [51]. Briefly, a culture medium containing a starting inoculum of $5.0 \times 10^6$ CFU/mL of strain VA-416/02 was incubated aerobically at 35 °C under orbital agitation (200 rpm) in Mueller-Hinton broth, in the absence and presence of 2 μg/mL meropenem and 32 μg/mL inhibitor. Bacterial count (expressed in CFU/mL) in the control and antibiotic-containing media was determined every hour for up to 6 h of incubation, by serial 10-fold dilution and direct plating of 0.1 mL of the sample on Mueller-Hinton Agar medium (without antibiotic), incubated for 24 h at 35 °C.

*4.2.3 Inhibition of human glyoxalase II (hGloII)*

The assay was performed as previously described [41]. Briefly, the activity of recombinant hGloII [57] was measured by following the disappearance of its substrate *S*-D-lactoylglutathione (Sigma, $\varepsilon_{240nm} = 3.1\ mM^{-1}cm^{-1}$) at 25 °C in 100 mM 4-morpholinopropane sulfonate (MOPS) buffer, pH 7.2 and with a Thermo Evolution spectrophotometer. The inhibitor, dissolved in DMSO was added to the assay mixture containing the substrate and the

reaction was started with enzyme (5-25 nM hGloII). All experiments were carried out in duplicate.

*4.2.4. Cell toxicity*

The potential cytotoxic activity of compounds was first evaluated using the commercially available integrity assay (CytoTox 96® non-radioactive cytotoxicity assay, Promega). The compounds were tested for their ability to induce the lysis of HeLa cells by measuring the release of lactate dehydrogenase (LDH) after incubating the HeLa cell cultures (20,000 cells/well) for 24h (37 °C, 5% $CO_2$) in DMEM (Dulbecco's Modified Eagle Medium) supplemented with 10% fetal bovine serum, 4.5 mg/mL glucose and 2 mM L-glutamine in the absence and presence of varying concentrations of the compounds (up to 250 µM). Further controls included samples containing the medium only or in which cell lysis was induced by the addition of 9% Triton X-100 (maximum LDH release control). The percentage of cytotoxicity was computed as 100 x (sample LDH release)/(maximum LDH release). The variation of the percentage of cytotoxicity allowed to compute an $IC_{50}$ value (compound concentration inducing 50% cytoxicity).

The cytotoxicity of the compounds was also calculated by measuring the number of viable cells in culture with respect to the control culture (cells treated with DMSO only) using the RealTime-Glo™ MT Cell Viability Assay, in the absence and presence of varying concentrations of the inhibitors. The assay is a nonlytic, homogeneous, bioluminescent method to measure cell viability/proliferation in real time using NanoLuc® luciferase and a cell-permeant prosubstrate (MT Cell Viability Substrate). The potential cytotoxicity was tested by incubating the compounds with Hela cells (1500 cells/well) for up to 48 h in DMEM. Both HeLa and A549 (adenocarcinomic human alveolar basal epithelial cells) human cell lines were used in these experiments.

The cytotoxicity of selected compounds was also assessed on normal human cells, Peripheral Blood Mononucleated Cells (PBMC). PBMC were prepared from four buffy coats from individual donors of the « Etablissement Francais du Sang » (EFS). Leukocytes were purified by density-based centrifugation using Histopaque 1077 (Sigma-Aldrich) and frozen. After thawing, PBMC were resuspended at 1.10e6/mL in RPMI medium supplemented with 10% FBS and 50 µL distributed in 96 well plates. The compounds, resuspended at 20 mM in DMSO, were diluted at 1 mM in RPMI before serial dilution in RPMI. 50 µL of the diluted compounds were then added to the wells containing the cells, in duplicate. The final concentrations of

compounds was ranging from 500 μM to 7.8 μM. After 24 hours, cells were analyzed by cytometry using a Novocyte Flow Cytometer. Live cells were identified using a FSC/SSC gating. $IC_{50}$ values were calculated using GraphPad Prims version 9 (Table S6).

*4.3. X-ray crystallography section*

VIM-2 was expressed and purified following established protocols [53,58]. Crystals of the enzyme were grown within a few days using the sitting drop vapor diffusion method [59] at room temperature, as described elsewhere [53,58]. Soaking solutions for compounds **8**, **10**, and **14**, formerly dissolved in dimethyl sulfoxide (DMSO), were prepared by dilution in PEG-400 using a 1:9 molar ratio (final concentration 5 mM). Each enzyme-inhibitor complex was obtained by adding 1 μL of soaking solution to the crystallization drop containing preformed crystals and allowing compound diffusion for 30 minutes at room temperature. Crystals were then frozen in liquid nitrogen. Diffraction data were collected at 100 K using synchrotron radiation at the Diamond Light Source (DLS, UK) beamline I04 equipped with an Eiger2 XE 16M detector. Reflections were integrated using XDS [60] and scaled with SCALA [61] from the CCP4 suite [62]. The structures were solved by molecular replacement using MOLREP [63] and the structure of VIM-2 (PDB code 6SP7 [34]), as search model (excluding non-protein atoms and water molecules). The three structures were refined using REFMAC5 from the CCP4 suite [64]. The molecular graphic software Coot [65] was used for manual rebuilding and modelling of missing atoms in the electron density and to add solvent molecules. In each structure, the inspection of the Fourier difference map clearly evidenced the presence of the inhibitor inside the catalytic cavity that was modelled accordingly. The occupancy of the exogenous ligands was adjusted and refined to values resulting in atomic displacement parameters close to those of neighboring protein atoms in fully occupied sites. The final models were inspected manually and checked with Coot [65] and PROCHECK [66]. Structural figures were generated using the molecular graphic software CCP4mg [67]. Data collection, processing, and refinement statistics are summarized in Table S1. Final coordinates and structure factors were deposited in the Protein Data Bank (PDB) under the codes 7OVF (VIM-2/**8**), 7OVE (VIM-2/**10**), and 7OVH (VIM-2/**14**).

*4.4. Equilibrium dialysis and native state electrospray ionization mass spectrometry*

These studies have been performed on compound **6** following published procedures [47]. The equilibrium dialysis experiment is briefly described in the Supplementary Material part.

## Declaration of competing interest

The authors declare that they have no competing financial interests or personal relationships that could have appeared to influence the work reported in this paper.


## Acknowledgements

Part of this work was supported by *Agence Nationale de la Recherche* (ANR-14-CE16-0028-01), the *Deutsche Forschungsgemeinschaft* (BE1540/15-2 within SPP 1710 to K.B.). We thank Mr Pierre Sanchez for mass spectrometry analyses. We also thank the Diamond Light Source for providing us beamtime (BAG proposal MX21741) and the staff of beamline I04 for their assistance with crystal testing and data collection. The Dipartimento di Biotecnologie Mediche and the Dipartimento di Biotecnologie, Chimica e Farmacia, University of Siena, were both awarded "Department of Excellence 2018-2022" by the Italian Ministry of Education, University and Research (MIUR, L. 232/2016).


## Appendix A. Supplementary data

Supplementary data can be found online at…
General synthetic procedures (Schemes S1 and S2). Characterization of final compounds. X-ray crystallography (Table S1 and Figure S1). Figure S2 and Tables S2-S5 showing results of microbiological assays. Experimental details for equilibrium dialysis and native state ESI-MS studies (Figures S3 and S4). Cytotoxicity toward PBMC (Table S6). $^{1}H$ and $^{13}C$ NMR spectra and chromatographic profile of final compounds.
X-ray structures of VIM-2/inhibitor complexes: PDB codes 7OVF (cpd **8**), 7OVE (cpd **10**), 7OVH (cpd **14**): Authors will release the atomic coordinates and experimental data upon article publication.

## References


[1] C. Lee Ventola, The antibiotic resistance crisis: part1: causes and threats, Pharm. Ther. 40 (2015) 277-283. PMC4378521

[2] W. C. Reygaert, An overview of the antimicrobial resistance mechanisms of bacteria, AIMS Microbiol. 4 (2018) 482-501. DOI: 10.3934/microbiol.2018.3.482

[3] A. Cassini, L. D. Högberg, D. Plachouras, A. Quattrocchi, A. Hoxha, G. S. Simonsen, M. Colomb-Cotinat, M. E. Kretzschmar, B. Devleesschauwer, M. Cecchini, D. A. Ouakrim, T. C. Oliveira, M. J. Struelens, C. Suetens, D. L. Monnet, Burden of AMR Collaborative Group. Attributable deaths and disability-adjusted life-years caused by infections with antibiotic-resistant bacteria in the EU and the European Economic Area in 2015: a population-level modelling analysis, Lancet Infect. Dis. 19 (2019) 56-66. DOI: 10.1016/S1473-3099(18)30605-4

[4] World Health Organization, Global priority list of antibiotic-resistant bacteria to guide research, discovery and development of new antibiotics, 27 february 2017.

[5] T. R. Walsh, M. A. Toleman, The emergence of pan-resistant Gram-negative pathogens merits a rapid global political response, J. Antimicrob. Chemother. 67 (2012) 1-3. DOI: 10.1093/jac/dkr378

[6] P. Nordmann, T. Naas, L. Poirel, Global spread of carbapenemase-producing Enterobacteriaceae, Emerg. Infect. Dis. 17 (2011) 1791-1798. DOI: 10.3201/eid1710.110655

[7] K. Bush, Past and present perspectives on β-lactamases, Antimicrob. Agents Chemother. 62 (2018) e01076-18. DOI: 10.1128/AAC.01076-18

[8] S. E. Boyd, D. M. Livermore, D. C. Hooper, W. W. Hope, Metallo-β-lactamases: structure, function, epidemiology, treatment options, and the development pipeline, Antimicrob. Agents Chemother. 64 (2020) e00397-20. DOI: 10.1128/AAC.00397-20

[9] G. Bahr, L. J. Gonzalez, A. J. Vila, Metallo-β-lactamase inhibitors in the age of multidrug resistance: from structure and mechanism to evolution, dissemination, and inhibitor design, Chem. Rev. 121 (2021) 7957-8094. DOI: 10.1021/acs.chemrev.1c00138

[10] V. R. Gajamer, A. Bhattacharjee, D. Paul, C. Deshamukhya, A. K. Singh, N. Pradhan, H. K. Tiwari, *Escherichia coli* encoding $bla_{NDM-5}$ associated with community-acquired urinary tract infections with unusual MIC creep-like phenomenon against imipenem, J. Glob. Antimicrob. Resist. 14 (2018) 228-232. DOI: 10.1016/j.jgar.2018.05.004

[11] C. Gonzalez-Bello, D. Rodriguez, M. Pernas, A. Rodriguez, E. Colchon, β-Lactamase inhibitors to restore the efficacy of antibiotics against superbugs, J. Med. Chem. 63 (2020) 1859-1881. DOI: 10.1021/acs.jmedchem.9b01279

[12] J. C. Vazquez-Ucha, J. Arca-Suarez, G. Bou, A. Beceiro, New carbapenemase inhibitors : clearing the way for the β-lactams, Int. J. Mol. Sci. 21 (2020) 9308. DOI: 10.3390/ijms21239308

[13] J.-D. Docquier, S. Mangani, An update on β-lactamase inhibitor discovery and development, Drug Resist. Updat. 36 (2018) 13-29. DOI: 10.1016/j.drup.2017.11.002

[14] L. C. Ju, Z. Cheng, W. Fast, R. A. Bonomo, M. W. Crowder, The continuing challenge of metallo-β-lactamase inhibition: mechanism matters, Trends Pharmacol. Sci. 39 (2018) 635-647. DOI: 10.1016/j.tips.2018.03.007

[15] A. R. Palacios, M.-A. Rossi, G. S. Mahler, A. J. Vila, Metallo-β-lactamase inhibitors inspired on snapshots from the catalytic mechanism, Biomolecules 10 (2020) 854. DOI: 10.3390/biom10060854

[16] A. Y. Chen, R. N. Adamek, B. L. Dick, C. V. Credille, C. N. Morrison, S. M. Cohen, Targeting metalloenzymes for therapeutic intervention, Chem. Rev. 119 (2019) 1323-1455. DOI: 10.1021/acs.chemrev.8b00201

[17] M. M. Gonzalez, M. Kosmopoulou, M. F. Mojica, V. Castillo, P. Hinchliffe, I. Pettinati, J. Brem, C. J. Schofield, G. Mahler, R. A. Bonomo, L. I. Llarrull, J. Spencer, A. J. Vila, Bisthiazolidines: a substrate-mimicking scaffold as an inhibitor of the NDM-1 carbapenemase, ACS Inf. Dis. 1 (2015) 544-554. DOI: 10.1021/acsinfecdis.5b00046

[18] F. M. Klingler, T. A. Wichelhaus, D. Frank, J. Cuesta-Bernal, J. El-Delik, H. Florian Müller, H. Sjuts, S. Göttig, A. Koenigs, K. M. Pos, D. Pogoryelov, E. Proschak, Approved drugs containing thiols as inhibitors of metallo-β-lactamases: strategy to combat multidrug-resistant bacteria, J. Med. Chem. 58 (2015) 3626-3630. DOI: 10.1021/jm501844d

[19] K. H. M. E. Tehrani, N. I. Martin, Thiol-containing metallo-β-lactamase inhibitors resensitize resistant Gram-negative bacteria to meropenem, ACS Inf. Dis. 3 (2017) 711-717. DOI: 10.1021/acsinfecdis.7b00094

[20] S. Liu, L. Jing, Z.-J. Yu, C. Wu, Y. Zheng, E. Zhang, Q. Chen, Y. Yu, L. Guo, Y. Wu, G.-B. Li, ((S)-3-Mercapto-2-methylpropanamido)acetic acid derivatives as metallo-β-lactamase inhibitors: synthesis, kinetic and crystallographic studies, Eur. J. Med. Chem. 145 (2018) 649-660. https://doi.org/10.1016/j.ejmech.2018.01.032

[21] J. Brem, S. S. van Berkel, WS. Aik, A. M. Rydzik, M. B. Avison, I. Pettinati, K.-D. Umland, A. Kawamura, J. Spencer, T. D. W. Claridge, M. A. McDonough, C. J. Schofield,

Rhodanine hydrolysis leads to potent thioenolate mediated metallo-β-lactamase inhibition, Nat. Chem. 6 (2014) 1084-1090. DOI: 10.1038/nchem.2110

[22] Y. Xiang, C. Chen, W.-M. Wang, L.-W. Xu, K.-W. Yang, P. Oelschlaeger, Y. He, Rhodanine as a potent scaffold for the development of broad-spectrum metallo-β-lactamase inhibitors, ACS Med. Chem. Lett. 9 (2018) 359-364. DOI: 10.1021/acsmedchemlett.7b00548

[23] A. Y. Chen, P. W. Thomas, A. C. Stewart, A. Bergstrom, Z. Cheng, C. Miller, C. R. Bethel, S. H. Marshall, C. V. Credille, C. L. Riley, R. C. Page, R. A. Bonomo, M. W. Crowder, D. L. Tierney, W. Fast, S. M. Cohen, Dipicolinic acid derivatives as inhibitors of New Delhi Metallo-β-lactamase-1, J. Med. Chem. 60 (2017) 7267-7283. DOI: 10.1021/acs.jmedchem.7b00407

[24] A. M. King, S. A. Reid-Yu, W. Wang, D. T. King, G. De Pascale, N. C. Strynadka, T. R. Walsh, B. K. Coombes, G. D. Wright, Aspergillomarasmine A overcomes metallo-β-lactamase antibiotic resistance, Nature, 510 (2014) 503-506. DOI: 10.1038/nature13445

[25] O. Samuelsen, O. A. H. Astrand, C. Fröhlich, A. Heikal, S. Skagseth, T. J. O. Carlsen, H. S. Leiros, A. Bayer, C. Schnaars, G. Kildahl-Andersen, S. Lauksund, S. Finke, S. Huber, T. Gjoen, A. M. S. Andresen, O. A. Okstad, P. Rongved, ZN148 – a modular synthetic metallo-β-lactamase inhibitor reverses carbapenem-resistance in Gram-negative pathogens *in vivo*, Antimicrob. Agents Chemother. 64 (2020) e02415-19. DOI: 10.1128/AAC.02415-19

[26] C. J. Burns, D. Daigle, B. Liu, D. McGarry, D. C. Pevear, R. E. Trout, β-Lactamase inhibitors. WO Patent WO 2014/ 089365 A1.

[27] Y. L. Wang, S. Liu, Z.-J. Yu, Y. Lei, M.-Y. Huang, Y.-H. Yan, Q. Ma, Y. Zheng, H. Deng, Y. Sun, C. Wu, Y. Yu, Q. Chen, Z. Wang, Y. Wu, G.-B. Li, Structure-based development of (1-(3'-mercaptopropanamido)methyl)boronic acid derived broad-spectrum, dual-action inhibitors of metallo- and serine-β-lactamases, J. Med. Chem. 62 (2019) 7160-7184. DOI: 10.1021/acs.jmedchem.9b00735

[28] S. J. Hecker, K. R. Reddy, O. Lomovskaya, D. C. Griffith, D. Rubio-Aparicio, K. Nelson, R. Tsivkovski, D. Sun, M. Sabet, Z. Tarazi, J. Parkinson, M. Totrov, S. H. Boyer, T. W. Glinka, O. A. Pemberton, Y. Chen, M. N. Dudley, Discovery of cyclic boronic acid QPX7728, an ultra-broad-spectrum inhibitor of serine and metallo-β-lactamases, J. Med. Chem. 63 (2020) 7491-7507. DOI: 10.1021/acs.jmedchem.9b01976

[29] A. Parkova, A. Lucic, A. Krajnk, J. Brem, K. Calvopina, G. W. Langley, M. A. McDonough, P. Trapencieris, C. J. Schofield, Broad spectrum β-lactamase inhibition by a

thioether substituted bicyclic boronate, ACS Inf. Dis. 6 (2020) 1398-1404. DOI: 10.1021/acsinfecdis.9b00330

[30] O. A. Pemberton, P. Jaishankar, A. Akhtar, J. L. Adams, L. N. Shaw, A. R. Renslo, Y. Chen, Heteroaryl phosphonates as non covalent inhibitors of both serine- and metallocarbapenemases, J. Med. Chem. 62 (2019) 8480-8496. DOI: 10.1021/acs.jmedchem.9b00728

[31] E. Romero, S. Oueslati, M. Benchekroun, A. C. A. D'Hollander, S. Ventre, K. Vijayakumar, C. Minard, C. Exilie, L. Tlili, P. Retailleau, A. Zavala, E. Elisée, E. Selwa, L. A. Nguyen, A. Pruvost, T. Naas, B. I. Iorga, R. H. Dodd, K. Cariou, Azetidinimines, as a novel series of non-covalent broad-spectrum inhibitors of β-lactamases with submicromolar activities against carbapenemases KPC-2 (class A), NDM-1 (class B) and OXA-48 (class D), Eur. J. Med Chem. 219 (2021) 113418. DOI: 10.1016/j.ejmech.2021.113418

[32] N. Reddy, M. Shungube, P. I. Arvidsson, S. Baijnath, H. G. Kruger, T. Govender, T. Naicker, A 2018-2019 patent review of metallo-β-lactamase inhibitors, Exp. Opin. Ther. Pat. 30 (2020) 541-555. DOI: 10.1080/13543776.2020.1767070

[33] D. T. Davies, S. Leiris, N. Sprynski, J. Castandet, C. Lozano, J. Bousquet, M. Zalacain, S. Vasa, P. K. Dasari, R. Pattipati, N. Vempala, S. Gujjewar, S. Godi, R. Jallala, R. R. Sathyap, N. A. Darshanoju, V. R. Ravu, R. R. Juventhala, N. Pottabathini, S. Sharma, S. Pothukanuri, K. Holden, P. Warn, F. Marcoccia, M. Benvenuti, C. Pozzi, S. Mangani, J.-D. Docquier, M. Lemonnier, M. Everett, ANT2681: SAR studies leading to the identification of a metallo-lactamase inhibitor with potential for clinical use in combination with meropenem for the treatment of infections caused by NDM-producing Enterobacteriaceae, ACS Infect. Dis. 6 (2020) 2419-2430. DOI: 10.1021/acsinfecdis.0c00207

[34] B. Liu, R. E. L. Trout, G. H. Chu, D. McGarry, R. W. Jackson, J. C. Hamrick, D.M. Daigle, S. M. Cusick, C. Pozzi, F. De Luca, M. Benvenuti, S. Mangani, J.-D. Docquier, W. J. Weis, D. C. Pevear, L. Xerri, C. J. Burns, Discovery of Taniborbactam (VNRX-5133): a broad spectrum serine- and metallo-β-lactamase inhibitor for carbapenem-resistant bacterial infections, J. Med. Chem. 63 (2020) 2789-2801. DOI: 10.1021/acs.jmedchem.9b01518

[35] J. Brem, R. Cain, S. Cahill, M. A. McDonough, I. J. Clifton, J. C. Jiménez-Castellanos, M. B. Avison, J. Spencer, C. W. Fishwick, C. J. Schofield, Structural basis of metallo-β-lactamase, serine-β-lactamase and penicillin-binding protein inhibition by cyclic boronates, Nat. Commun. 7 (2016) 12406. DOI: 10.1038/ncomms12406

[36] L. Nauton, R. Kahn, G. Garau, J.-F. Hernandez, O. Dideberg, Structural insights into the design of inhibitiors of the L1 metallo-β-lactamase from *Stenotrophomonas maltophilia*, J. Mol. Biol. 375 (2008) 257-269. DOI: 10.1016/j.jmb.2007.10.036

[37] L. Olsen, S. Jost, H. W. Adolph, I. Pettersson, L. Hemmingsen, F. S. Jørgensen, New leads of metallo-β-lactamase inhibitors from structure-based pharmacophore design, Bioorg. Med. Chem. 14 (2006) 2627-2635. DOI: 10.1016/j.bmc.2005.11.046

[38] P. Vella, W. M. Hussein, E. W. Leung, D. Clayton, D. L. Ollis, N. Mitić, G. Schenk, R. P. McGeary, The identification of new metallo-β-lactamase inhibitor leads from fragment-based screening, Bioorg. Med. Chem. Lett. 21 (2011) 3282-3285. DOI: 10.1016/j.bmcl.2011.04.027

[39] T. Christopeit, T. J. Carlsen, R. Helland, H. K. Leiros, Discovery of novel inhibitor scaffolds against the metallo-β-lactamase VIM-2 by surface plasmon resonance (SPR) based fragment screening, J. Med Chem. 58 (2015) 8671-8682. DOI: 10.1021/acs.jmedchem.5b01289

[40] F. Spyrakis, G. Celenza, F. Marcoccia, M. Santucci, S. Cross, P. Bellio, L. Cendron, M. Perilli, D. Tondi, Structure-based virtual screening for the discovery of novel inhibitors of New Delhi Metallo-β-lactamase-1, ACS Med. Chem. Lett. 9 (2018) 45-50. DOI: 10.1021/acsmedchemlett.7b00428

[41] L. Gavara, L. Sevaille, F. De Luca, P. Mercuri, C. Bebrone, G. Feller, A. Legru, G. Cerboni, S. Tanfoni, D. Baud, G. Cutolo, B. Bestgen, G. Chelini, F. Verdirosa, F. Sannio, C. Pozzi, M. Benvenuti, K. Kwapien, M. Fischer, K. Becker, J.-M. Frère, S. Mangani, N. Gresh, D. Berthomieu, M. Galleni, J.-D. Docquier, J.-F. Hernandez, 4-Amino-1,2,4-triazole-3-thione-derived Schiff bases as metallo-β-lactamase inhibitors, Eur. J. Med. Chem. 208 (2020) 112720. DOI: 10.1016/j.ejmech.2020.112720

[42] F. Spyrakis, M. Santucci, L. Maso, S. Cross, E. Gianquinto, F. Sannio, F. Verdirosa, F. De Luca, J.-D. Docquier, L. Cendron, D. Tondi, A. Venturelli, G. Cruciani, M. P. Costi, Virtual screening identifies broad-spectrum β-lactamase inhibitors with activity on clinically relevant serine- and metallo-carbapenemases, Sci. Rep. 10 (2020) 12763. DOI: 10.1038/s41598-020-69431-y

[43] L. Sevaille, L. Gavara, C. Bebrone, F. De Luca, L. Nauton, M. Achard, P. Mercuri, S. Tanfoni, L. Borgianni, C. Guyon, P. Lonjon, G. Turan-Zitouni, J. Dzieciolowski, K. Becker, L. Bénard, C. Condon, L. Maillard, J. Martinez, J.-M. Frère, O. Dideberg, M. Galleni, J.-D.

Docquier, J.-F. Hernandez, 1,2,4-Triazole-3-thione compounds as inhibitors of dizinc metallo-β-lactamase, ChemMedChem 12 (2017) 972-985. DOI: 10.1002/cmdc.201700186

[44] L. Gavara, F. Verdirosa, A. Legru, P. S. Mercuri, L. Nauton, L. Sevaille, G. Feller, D. Berthomieu, F. Sannio, F. Marcoccia, S. Tanfoni, F. De Luca, N. Gresh, M. Galleni, J.-D. Docquier, J.-F. Hernandez, 4-(N-Alkyl- and -acyl-amino)-1,2,4-triazole-3-thione analogs as metallo-β-lactamase inhibitors: impact of 4-linker on potency and spectrum of inhibition, Biomolecules 10 (2020) 1094. DOI: 10.3390/biom10081094

[45] L. Gavara, A. Legru, F. Verdirosa, L. Sevaille, L. Nauton, G. Corsica, P. S. Mercuri, F. Sannio, G. Feller, R. Coulon, F. De Luca, G. Cerboni, S. Tanfoni, G. Chelini, M. Galleni, J.-D. Docquier, J.-F. Hernandez, 4-Alkyl-1,2,4-triazole-3-thione analogues as metallo-β-lactamase inhibitors, Bioorg. Chem. 113 (2021) 105024. 10.1016/j.bioorg.2021.105024

[46] R. F. Deprez-Poulain, J. Charton, V. Leroux, B. P. Deprez, Convenient synthesis of 4*H*-1,2,4-triazole-3-thiols using di-2-pyridylthionocarbamate,Tetrahedron Lett. 48 (2007) 8157-8162. https://doi.org/10.1016/j.tetlet.2007.09.094

[47] C. A. Thomas, Z. Cheng, K. Yang, E. Hellwarth, C. J. Yurkiewicz, F. M. Baxter, S. A. Fullington, S. A. Klinsky, J. L. Otto, A. Y. Chen, S. M. Cohen, M. W. Crowder, Probing the mechanism of inhibition for various inhibitors of metallo-β-lactamases VIM-2 and NDM-1, J. Inorg. Biochem. 210 (2020) 111123. DOI: 10.1016/j.jinorgbio.2020.111123

[48] L. Huang, J. Haagensen, D. Verotta, P. Lizak, F. Aweeka, K. Yang, Determination of meropenem in bacterial media by LC-MS/MS, J. Chromatogr. B Analyt. Technol. Biomed. Life Sci. 961 (2014) 71-76. DOI: 10.1016/j.jchromb.2014.05.002

[49] G. Landini, T. Di Maggio, F. Sergio, J.-D. Docquier, G. M. Rossolini, L. Pallecchi, Effect of high *N*-acetylcysteine concentrations on antibiotic activity against a large collection of respiratory pathogens, Antimicrob. Agents Chemother. 60 (2016) 7513-7517. DOI: 10.1128/AAC.01334-16

[50] M. J. Hall, R. F. Middleton, D. Westmacott, The fractional inhibitory concentration (FIC) index as a measure of synergy, J. Antimicrob. Chemother. 11 (1983) 427-433. DOI: 10.1093/jac/11.5.427

[51] European Committee for Antimicrobial Susceptibility Testing (EUCAST) of the European Society of Clinical Microbiology and Infectious Dieases (ESCMID), EUCAST Definitive Document E.Def 1.2, May 2000: Terminology relating to methods for the determination of

susceptibility of bacteria to antimicrobial agents, Clin Microbiol Infect. 6 (2000) 503-508. DOI: 10.1046/j.1469-0691.2000.00149.x

[52] C. Mugnaini, F. Sannio, A. Brizzi, R. Del Prete, T. Simone, T. Ferraro, F. De Luca, F. Corelli, J.-D. Docquier, Screen of unfocused libraries identifies compounds with direct or synergistic antibacterial activity, ACS Med. Chem. Lett. 11 (2020) 899-905. 10.1021/acsmedchemlett.9b00674

[53] J.-D. Docquier, J. Lamotte-Brasseur, M. Galleni, G. Amicosante, J. M. Frère, G. M. Rossolini, On functional and structural heterogeneity of VIM-type metallo-β-lactamases, J. Antimicrob. Chemother. 51 (2003) 257-266. DOI: 10.1093/jac/dkg067

[54] Clinical Laboratory Standard Institute, Methods for dilution antimicrobial susceptibility tests for bacteria that grow aerobically, Document M07-A10, 2015, Twelfth Edition, Wayne, PA, USA.

[55] S. Cagnacci, L. Gualco, S. Roveta, S. Mannelli, L. Borgianni, J.-D. Docquier, F. Dodi, M. Centanaro, E. Debbia, A. Marchese, G. M. Rossolini, Bloodstream infections caused by multidrug-resistant *Klebsiella pneumoniae* producing the carbapenem-hydrolysing VIM-1 metallo-β-lactamase: first Italian outbreak, J. Antimicrob. Chemother. 61 (2008) 296-300. DOI: 10.1093/jac/dkm471

[56] F. Luzzaro, J.-D. Docquier, C. Colinon, A. Endimiani, G. Lombardi, G. Amicosante, G. M. Rossolini, A. Toniolo, Emergence in *Klebsiella pneumoniae* and *Enterobacter cloacae* clinical isolates of the VIM-4 metallo-β-lactamase encoded by a conjugative plasmid, Antimicrob. Agents Chemother. 48 (2004) 648-650. DOI: 10.1128/AAC.48.2.648-650.2004

[57] M. Akoachere, R. Iozef, S. Rahlfs, M. Deponte, B. Mannervik, D. J. Creighton, H. Schirmer, K. Becker, Characterization of the glyoxalases of the malarial parasite Plasmodium falciparum and comparison with their human counterparts, Biol. Chem. 386 (2005) 41-52. DOI: 10.1515/BC.2005.006

[58] I. Garcia-Saez, J.-D. Docquier, G. M. Rossolini, O. Dideberg, The three-dimensional structure of VIM-2, a Zn-beta-lactamase from Pseudomonas aeruginosa in its reduced and oxidised form, J. Mol. Biol. 375 (2008) 604-611. 10.1016/j.jmb.2007.11.012

[59] M. Benvenuti, S. Mangani, Crystallization of soluble proteins in vapor diffusion for X-ray crystallography, Nat. Protoc. 2 (2007) 1633-1651. 10.1038/nprot.2007.198

[60] W. Kabsch, XDS, Acta Crystallogr. D Biol. Crystallog. 66 (2010) 125-132. 10.1107/S0907444909047337

[61] P. R. Evans, An introduction to data reduction: space-group determination, scaling and intensity statistics, Acta Crystallogr. D Biol. Crystallog. 67 (2011) 282-292. 10.1107/S090744491003982X

[62] M. D. Wynn, C. C. Ballard, K. D. Cowtan, E. J. Dodson, P. Emsley, P. R. Evans, R. M. Keegan, E. B. Krissinel, A. G. Leslie, A. McCoy, S. J. McNicholas, G. N. Murshudov, N. S. Pannu, E. A. Potterton, H. R. Powell, R. J. Read, A. Vagin, K. S. Wilson, Overview of the CCP4 suite and current developments, Acta Crystallogr. D Biol. Crystallogr. 67 (2011) 235-242. 10.1107/S0907444910045749

[63] A. Vagin, A. Teplyakov, Molecular replacement with MOLREP, Acta Crystallogr. D Biol. Crystallog. 66 (2010) 22-25. 10.1107/S0907444909042589

[64] G. N. Murshudov, P. Shubak, A. A. Lebedev, N. S. Pannu, R. A. Steiner, R. A. Nicholls, M. D. Winn, F. Long, A. A. Vagin, REFMAC5 for the refinement of macromolecular crystal structures, Acta Crystallogr. D Biol. Crystallogr. 67 (2011) 355-367. 10.1107/S0907444911001314

[65] P. Emsley, B. Lohkamp, W. G. Scott, K. Cowtan, Features and development of Coot, Acta Crystallogr. D Biol. Crystallogr. 66 (2010) 486-501. 10.1107/S0907444910007493

[66] R. A. Laskowski, M. W. MacArthur, D. S. Moss, J. M. Thornton, PROCHECK: a program to check the stereochemical quality of protein structures, J. Appl. Crystallog. 26 (1993) 283-291. https://doi.org/10.1107/S0021889892009944

[67] L. Potterton, S. McNicholas, E. Krissinel, J. Gruber, K. Cowtan, P. Emsley, G. N. Murshudov, S. Cohen, A. Perrakis, M. Noble, Developments in the CCP4 molecular-graphics project, Acta Crystallogr. D Biol. Crystallogr. 60 (2004) 2288-2294. 10.1107/S0907444904023716